

Photoacoustic imaging method based on arc-direction compressed sensing and multi-angle observation

Mingjian Sun,* Naizhang Feng, Yi Shen, Xiangli Shen, Liyong Ma, Jiangang Li and Zhenghua Wu

Department of Control Science and Engineering, Harbin Institute of Technology, Harbin 150001, China
summingjian@hit.edu.cn

Abstract: In photoacoustic imaging (PAI), the photoacoustic (PA) signal can be observed only from limit-view angles due to some structure limitations. As a result, data incompleteness artifacts appear and some image details lose. An arc-direction mask in PA data acquisition and arc-direction compressed sensing (CS) reconstruction algorithm are proposed instead of the conventional rectangle CS methods for PAI. The proposed method can effectively realize the compression of the PA data along the arc line and exactly recover the PA images from multi-angle observation. Simulation results demonstrate that it has the potential of application in high-resolution PAI for obtaining highly resolution and artifact-free PA images.

©2011 Optical Society of America

OCIS codes: (100.3020) Image reconstruction-restoration; (110.5120) Photoacoustic imaging; (170.5120) Photoacoustic imaging.

References and links

1. M. H. Xu and L. V. Wang, "Photoacoustic imaging in biomedicine," *Rev. Sci. Instrum.* **77**(4), 041101 (2006).
2. L. V. Wang, "Prospects of photoacoustic tomography," *Med. Phys.* **35**(12), 5758–5767 (2008).
3. H. F. Zhang, K. Maslov, M. Sivaramakrishnan, G. Stoica, and L. V. Wang, "Imaging of hemoglobin oxygen saturation variations in single vessels in vivo using photoacoustic microscopy," *Appl. Phys. Lett.* **90**(5), 053901 (2007).
4. R. I. Siphanto, K. K. Thumma, R. G. M. Kolkman, T. G. van Leeuwen, F. F. M. de Mul, J. W. van Neck, L. N. A. van Adrichem, and W. Steenbergen, "Serial noninvasive photoacoustic imaging of neovascularization in tumor angiogenesis," *Opt. Express* **13**(1), 89–95 (2005).
5. R. G. M. Kolkman, J. H. G. M. Klaessens, E. Hondebrink, J. C. W. Hopman, F. F. M. de Mul, W. Steenbergen, J. M. Thijssen, and T. G. van Leeuwen, "Photoacoustic determination of blood vessel diameter," *Phys. Med. Biol.* **49**(20), 4745–4756 (2004).
6. K. Homan, S. Kim, Y.-S. Chen, B. Wang, S. Mallidi, and S. Emelianov, "Prospects of molecular photoacoustic imaging at 1064 nm wavelength," *Opt. Lett.* **35**(15), 2663–2665 (2010).
7. A. De La Zerde, C. Zavaleta, S. Keren, S. Vaithilingam, S. Bodapati, Z. Liu, J. Levi, B. R. Smith, T. J. Ma, O. Oralkan, Z. Cheng, X. Y. Chen, H. J. Dai, B. T. Khuri-Yakub, and S. S. Gambhir, "Carbon nanotubes as photoacoustic molecular imaging agents in living mice," *Nat. Nanotechnol.* **3**(9), 557–562 (2008).
8. V. Torres-Zúñiga, R. Castañeda-Guzmán, S. J. Pérez-Ruiz, O. G. Morales-Saavedra, and M. Zepahua-Camacho, "Optical absorption photoacoustic measurements for determination of molecular symmetries in a dichroic organic-film," *Opt. Express* **16**(25), 20724–20733 (2008).
9. L. Li, R. J. Zemp, G. F. Lungu, G. Stoica, and L. V. Wang, "Photoacoustic imaging of lacZ gene expression in vivo," *J. Biomed. Opt.* **12**(2), 020504 (2007).
10. L. V. Wang, "Ultrasound-mediated biophotonic imaging: a review of acousto-optical tomography and photoacoustic tomography," *Dis. Markers* **19**(2-3), 123–138 (2003-2004).
11. C. Tao and X. J. Liu, "Reconstruction of high quality photoacoustic tomography with a limited-view scanning," *Opt. Express* **18**(3), 2760–2766 (2010).
12. K. Maslov, H. F. Zhang, S. Hu, and L. V. Wang, "Optical-resolution photoacoustic microscopy for in vivo imaging of single capillaries," *Opt. Lett.* **33**(9), 929–931 (2008).
13. J. Provost and F. Lesage, "The Application of Compressed Sensing for Photo-Acoustic Tomography," *IEEE T. Med. Imaging* **28**(4), 585–594 (2009).
14. D. Liang, H. F. Zhang, and L. Ying, "Compressed-Sensing Photoacoustic Imaging based on Random Optical Illumination," *Int. J. Funct. Inf. Personal. Med.* **2**(4), 394–406 (2009).
15. Z. Guo, C. Li, L. Song, and L. V. Wang, "Compressed sensing in photoacoustic tomography in vivo," *J. Biomed. Opt.* **15**(2), 021311 (2010).

16. M. H. Xu and L. V. Wang, "Time-domain Reconstruction for Thermoacoustic Tomography in a Spherical Geometry", *IEEE T. Med. Imaging*, **21**(7), 814–822 (2002).
17. D. L. Donoho, "Compressed sensing," *IEEE Trans. Inf. Theory* **52**(4), 1289–1306 (2006).
18. Y. Tsaig and D. L. Donoho, "Extensions of compressed Sensing," *Signal Process.* **86**(3), 549–571 (2006).

1. Introduction

During the past decade photoacoustic imaging (PAI) becomes a rapidly growing research area of biomedical applications [1]. Modern PAI manifests mostly in the form of photoacoustic tomography (PAT) [2], which is able to provide functional imaging of physiological parameters (such as the concentration and oxygen saturation of hemoglobin) [3–5], molecular imaging of biomarkers [6–8] and gene expression products [9]. The motivation of PAI is to combine optical and ultrasonic waves synergistically, providing the speckle-free imaging with high contrast and high resolution. In the most existing PAT systems, the high-resolution photoacoustic (PA) images require covering the entire surface of the tissue by an array of transducers [10–12]. In practice, it is almost impossible since the acoustic transducer arrays have the limited angular aperture.

To break the limitation, Jean Provost proposed a compressed sensing (CS) method, which testified that PA images are sparse and can be recovered from a small number of linear projections [13]. Liang Dong [14] and Zijian Guo [15] discussed the artifact generation and reduction of the limited-view imaging based on the CS method. From the literatures, the CS-PAI system can simplify the data acquisition (DAQ) equipment and obtain high resolution results with limit-view PA data.

However, the above results are still unsatisfactory with visible artifacts and loss of details [16]. In this paper, an arc-direction CS method is proposed which uses an arc-direction mask to realize the arc-direction data compression and reduces the arc artifacts by the multi-angle acoustic observation.

2. Methods

Figure 1 shows the schematic of the CS method for PAI with one ultrasonic transducer, which is an unfocused transducer (V323, Panametrics), with a central frequency of 2.25MHz, a nominal bandwidth of 1.5MHz, a opening angle of 90° and a diameter of 6 mm. The method requires an optical mask to realize random illumination in data acquisition and utilizes the sparsity of PA images in image reconstruction. A Q-switched Nd: YAG laser operates at 532 nm with pulse duration of 7 ns. The laser beam is expanded and homogenized to provide an incident energy density of 10 mJ/cm² on the tissue to be imaged. An optic mask is placed above the laser source and the tissue to carry out the laser encoded emission. The tissue is irradiated by the encoded laser light and absorbs the optic energy to generate the acoustic waves (Fig. 1 (a)).

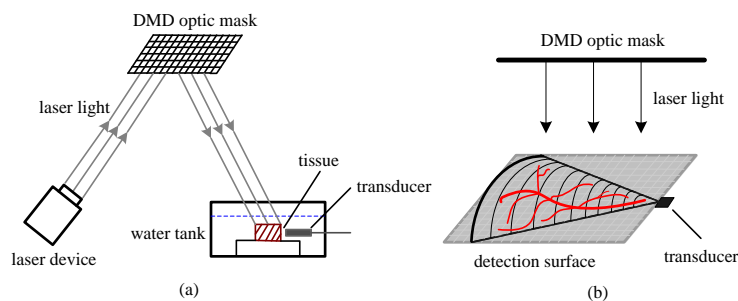


Fig. 1. The schematic of the CS method for PAI with one ultrasonic transducer. (a) Compressed data acquisition. (b) PA signals receiving

The transducer has a limited view which can be represented with a sector window. Therefore, the generated acoustic waves along the same arc line arrive at the transducer simultaneously, so the achieved signals are the information superposition along the arc-

direction. In addition, the single-element unfocused ultrasonic transducer can record the achieved PA signals for each mask pattern (Fig. 1(b)). Then the PA signals are collected in polar coordinates [REMOVED HYPERLINK FIELD] and indexed by radius R and angle θ . When the tissue is fully enclosed in the detection region, accurate recovery is possible from the sparse PA signal. Finally, a PA image can be reconstructed from the recorded PA signals by a suitable CS reconstruction algorithm. In the course, a scan conversion is required from polar coordinates to Cartesian coordinates.

In the process of compressed data acquisition, the objective for the use of arc-direction mask is to realize the compression of data along the arc line. The mask can be realized by digital micro-mirror device (DMD), which can reflect the short-pulsed laser light to the biological tissue. The mask spatial pattern can be modulated by the digital logical control circuit to create the time-varying switch array according to the binary Bernoulli random matrix. The mask changes its optical absorption-distribution pattern randomly for each laser light pulse. The Bernoulli random matrix is maximally incoherent with any sparsity transform, and therefore, it can be modeled as the random binary Bernoulli distribution-sparse measurement matrix to decide whether light passes through the mask.

Under practical conditions, the CS reconstruction quality mainly depends on the incoherence, numbers of masks and reconstruction algorithm [17]. In the process of PA image reconstruction, the forward problem that relates spatial electromagnetic (EM) absorption function x with measured PA signal values y can be described as $y = \Phi x$, where matrix Φ is the measurement matrix. Then the inverse problem can be described as $\hat{x} = \Phi^{-1} y$, where Φ^{-1} represents the inverse process, and \hat{x} is the reconstructed image.

If the measurement is incomplete, Φ is an ill-conditioned matrix and Φ^{-1} is not an exact inversion of Φ obviously. Intuitively, an incomplete data set will lead to uncertainties during the recovery of the signals. However, based on the CS theory, it is possible to reconstruct a K -sparse signal of length N from $O(K \log N)$ measurements. Suppose that measurement number is M and the measurement vector at the j -th arc position after M measurements is y_M^j , then the PA signal x^j can be reconstructed by Basis Pursuit denoising (BPDN) algorithm [18]:

$$\hat{x}^j = \arg \min \|x^j\|_1 \quad \text{subject to} \quad \|y_M^j - \Phi_{M \times N} x^j\|_2 \leq \varepsilon \quad (1)$$

Where x^j denotes the desired signal vector of length N at the j -th arc position, \hat{x}^j represents the reconstructed vector, $\Phi_{M \times N}$ is the random illumination matrix of M measurements, ε is a given noise level.

From the above descriptions, the PA data acquisition and image reconstruction are carried out along the arc-direction. Since the ultrasound transducer has its own opening angle, the PA signals outside the detecting area can't be detected in fact. In the existing CS method for PAI, the mask (shown in Fig. 2(a)) generates a rectangular measurement matrix with binary Bernoulli-distribution. When using the rectangle CS method, the measurement matrix is constructed in the whole rectangular area, so reconstructed artifacts ("+") generate outside the detecting area (shown in Fig. 2(c)).

To solve the problem, the measurement matrix should be suitably made for the detecting area with binary Bernoulli-distribution along the arc-direction (shown in Fig. 2(b)). When using the arc-direction CS method, the measurement matrix is made along the arc-direction, the matrix elements outside the sector window (detecting area) are constructed to zero ("0") and the matrix elements inside the sector window ("*") are constructed subject to binary Bernoulli distribution (shown in Fig. 2(d)).

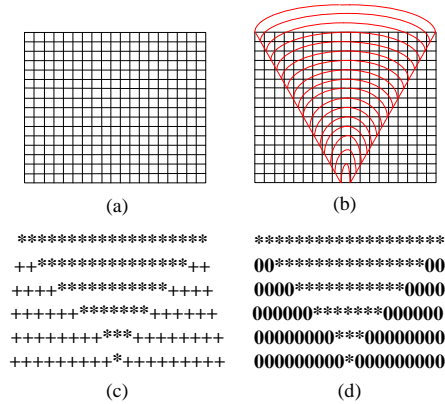


Fig. 2. Schematics of PA Images from different CS methods. (a) The rectangle mask. (b) The arc-direction mask. (c) PA image from the rectangle reconstruction algorithm. (d) PA image from the arc-direction reconstruction algorithm.

To evaluate the performance of the proposed method, reconstruction error E_R is defined as follows:

$$E_R = \frac{\|I_{CS} - I\|_2}{\|I\|_2} \quad (2)$$

Where I and I_{CS} respectively denotes the original and reconstructed image, $\|I\|_2$ denotes the two-norm of the image I .

3. Results and discussion

Reconstruction errors based on the rectangle CS and arc-direction CS method are shown in Fig. 3. A sparse phantom with 256×256 pixels is used in the simulation.

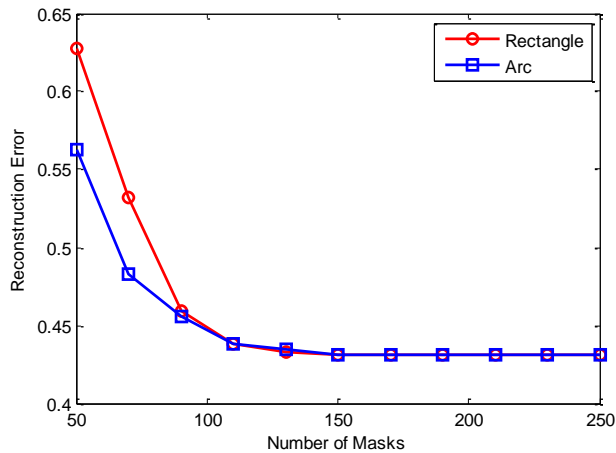


Fig. 3. Curves of reconstruction errors based on rectangle and arc-direction CS methods.

One unfocused single-element transducer is placed at the center of the virtual circular detection curve to acquire PA signals. When the number of masks is small, the rectangle CS performance is obviously worse than the arc-direction CS. When the number of masks is large enough (number > 120), reconstruction errors of the two CS methods becomes comparable.

Therefore, by using the proposed arc-direction CS method for PAI, fewer measurements and better performance are acquired.

However, the results from single transducer are still unsatisfactory with visible artifacts and loss of details. To solve the problem, four single-element transducers are adopted and placed at different degrees (0, 90, 180, 270 degree), which is shown in Fig. 4.

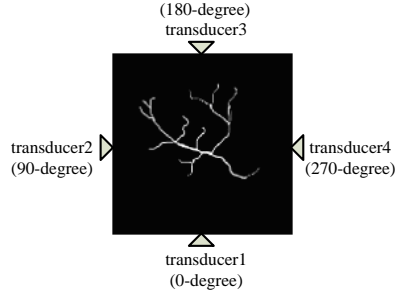


Fig. 4. Transducers' different observation locations using CS method for PAI based on multi-angle observation.

From every transducer, the phantom with 256×256 pixels is reconstructed respectively, and the results reconstructed by rectangle and arc-direction CS methods with 90 masks are shown in Fig. 5 (a)-(d) and (e)-(h), respectively. The images show that the results of the arc-direction CS method are superior to those of the rectangle CS method. For different-angle observations, the artifacts appear at different positions. Therefore, the image quality can be improved by fusing the reconstructed PA images from different observation angles.

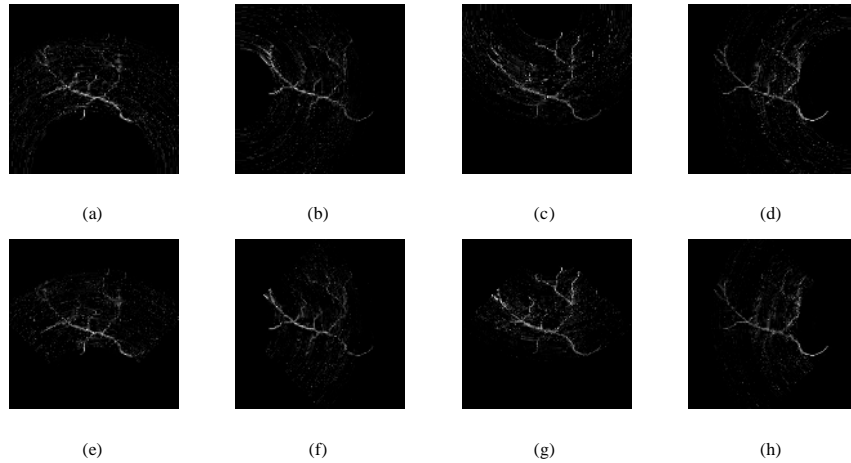


Fig. 5. Reconstruction of PA Images from different view degrees with 90 masks. (a)-(d) 0-degree, 90-degree, 180-degree and 270-degree using rectangle CS method respectively; (e)-(h) 0-degree, 90-degree, 180-degree and 270-degree using arc-direction CS method respectively.

The results are reconstructed by rectangle and arc-direction CS method based on multi-angle (90-degree separation between four transducers) observation with different masks are shown in Fig. 6 (a)-(c) and (d)-(f), respectively. The reconstruction errors of the rectangle and arc-direction CS method based on different observations respectively are shown in Fig. 7, which includes the reconstruction errors of the 0-degree, 90-degree, 180-degree, 270-degree and multi-angle observation. From the sub-images and curves, it demonstrates that the arc-direction method still shows better performance than the rectangle method under multi-angle observation. The multi-angle observation is sufficient for high-quality reconstruction, because its reconstruction error is much smaller than other observations. The comparison demonstrates

the multi-angle observation can reduce the number of masks needed for satisfying performances. So the arc-direction method based on multi-angle observation has the potential of application in high-resolution PAI for obtaining highly resolution and artifact-free PA images.

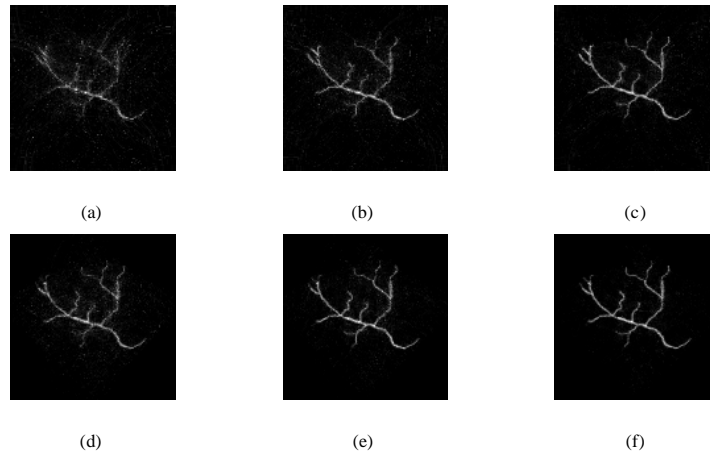


Fig. 6. Reconstruction of PA Images from multi-angle observation. (a)-(c) 90 masks, 150 masks and 210 masks using rectangle CS method respectively; (d)-(f) 90 masks, 150 masks and 210 masks using arc-direction CS method respectively.

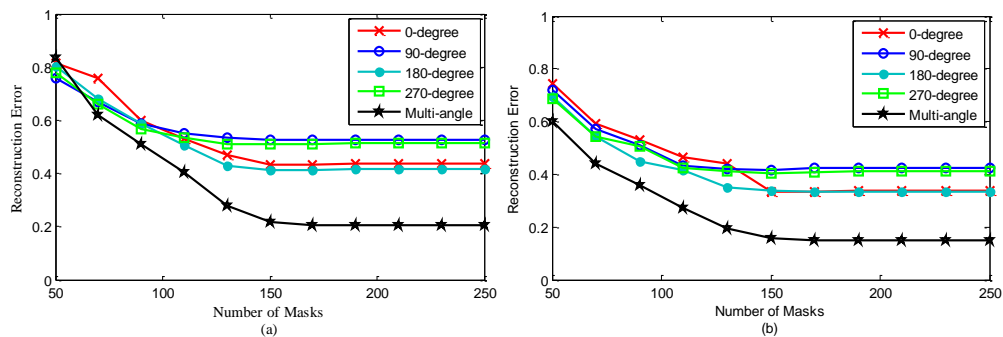


Fig. 7. Reconstruction errors using different observations. (a) Rectangle CS method. (b) Arc-direction CS method

In order to reach the higher resolution, more observations are required, which can lead to use more acquisition time and more transducers. So a suitable method should have the balance the compromise of the spatial resolution and the time resolution, and the proposed method can achieve the satisfying result performance using fewer masks and fewer transducers.

5. Conclusion

In summary, a PA imaging method based on arc-direction compressed sensing and multi-angle observation is proposed. The method utilizes an arc-direction mask to realize the compression of the PA data along the arc and exactly recover the PA images from multi-angle observation. Simulation shows that the proposed method can effectively eliminate the artifacts to improve the spatial resolution of PAI and can effectively reduce the measurement number to improve the time resolution.

Acknowledgement

This research is supported by the National Natural Science Foundation of China (30800240), Promotive Research Fund for Excellent Young and Middle-aged Scientists of Shandong Province (BS2010DX001) and Science & Technology Development Project of Weihai City (2010-3-96).